J. Fluid Mech. (2002), *vol.* 457, *pp.* 325–337.
DOI: 10.1017/S0022112001007686 Printed in the United Kingdom

Limiting maximum drag-reduction asymptote for the moment coefficient of a rotating disk in drag-reducing surfactant solution

By SATOSHI OGATA AND KEIZO WATANABE

Department of Mechanical Engineering, Graduate School of Engineering,
Tokyo Metropolitan University Minami Ohsawa, Hachiooji-shi,
Tokyo, 192-0397, Japan
ogata-satoshi@c.metro-u.ac.jp

(Received 8 February 2001 and in revised form 19 October 2001)

In this study, the limiting maximum drag-reduction asymptote for the moment coefficient of a rotating disk in a surfactant solution was obtained analytically. The analysis, which was based on the logarithmic velocity profile of turbulent pipe flow in the surfactant solution, was carried out using momentum integral equations of the boundary layer, and the moment coefficient results agreed with experimental results for maximum drag reduction in surfactant solution. Additionally, flow visualization was performed using the tracer and the tuft techniques, which revealed that the direction of flow of surfactant solution on the disk was turned towards the circumferential direction and the amplitude of the circular vortex on the rotating disk was reduced by addition of surfactant solution. The experimental results for flow angle on a rotating disk can be explained well with the analytical results.

1. Introduction

The drag reduction of surfactant solutions has attracted considerable attention from the point of view of energy conservation because mechanical degradation does not occur and the drag reduction ratio is higher than for polymer solutions in certain cocentration ranges (Zakin & Chang 1974; Ohlendorf, Interthal & Hoffmann 1986). Thus, many studies on drag reduction of surfactant solution have been conducted for an internal flow (Bewersdorff & Ohlendorf 1988; Warholic, Schmidt & Hanratty 1999; Zakin, Myska & Chara 1996). With regard to the mechanism of drag reduction due to a surfactant solution, Ito, Imao & Sugiyama (1995) investigated the characteristics of low-speed streaks in turbulent channel flow of surfactant solutions by the hydrogen-bubble flow visualization technique and clarified that the non-dimensional wall-normal distance of the centre of streamwise vortices was greater in flows with a large drag reduction ratio compared with that in Newtonian fluid flow. Kawaguchi *et al.* (1996) found using LDV techniques that streamwise and tangential components of turbulent intensity and Reynolds shear stress of surfactant solutions increased near to the wall. Considering the physical properties of surfactant solutions, Usui, Ito & Saeki (1996) reported that the apparent viscosity of surfactant solution showed a significant dependence on temperature and approximated that of tap water in high-shear-rate regions.

On the other hand, in order to improve the energy efficiency of complete closed loop systems, it is necessary to reduce not only frictional losses but also power losses

in turbo-machinery with surfactant solutions. In general, the frictional resistance of an enclosed rotating disk is closely related to estimates of frictional losses due to the impeller in the turbo-machinery. Although it is important to calculate the drag reduction of the frictional resistance of a rotating disk by adding surfactant additives in order to reduce the power loss of the turbo-machinery, there have been few studies on the frictional resistance of a rotating disk in surfactant solutions. With regard to rotating disk flow, Ogata & Watanabe (1999) reported on the drag reduction of surfactant solutions for an enclosed rotating disk by measuring the torque acting on the disk. The test surfactant solution was Ethoquad O/12 with sodium salicylate. It was shown that the drag reduction of the surfactant solution was dependent on both solution concentration and temperature, and the maximum drag reduction ratio was approximately 30%.

It is necessary to estimate the minimum moment coefficient in practical applications of a rotating disk in a drag-reducing surfactant solution. Two analytical methods can be used to obtain the minimum values of frictional resistance of a rotating disk. The first method uses the Navier–Stokes equation; the second involves the application of the momentum integral equations for a boundary layer. The first method is not suitable for obtaining the moment coefficient of a rotating disk, since the rheological equation of surfactant solutions has not yet been derived. The second method is applicable, since analysis is possible if the velocity profiles of the boundary layer are known, and the logarithmic velocity profiles in pipe flow have been presented in many studies. Additionally, in the case of dilute polymer solutions, the final velocity profile for maximum drag reduction has been obtained (Virk, Mickley & Smith 1970). If the velocity profile in pipe flow can be used to obtain the moment coefficient of a rotating disk with maximum drag reduction, the results using the momentum integral equations for a boundary layer on a rotating disk can be used to estimate the limit of drag reduction due to surfactant solutions. As mentioned above, there are little data available pertaining to the velocity profile of a rotating disk flow in a surfactant solution at present.

The purpose of this study is to obtain the limiting maximum drag-reduction asymptote for the moment coefficient of a rotating disk in a surfactant solution. Analysis was carried out using momentum integral equations of the boundary layer on a rotating disk based on the logarithmic velocity profile of turbulent pipe flow in a surfactant solution. The experimental torque measurment and flow visualization results were used to confirm the validity of the analytical results, and the experimental results for the moment coefficient for maximum drag reduction and the flow pattern could be explained well by the analytical results.

2. Analysis

2.1. *Moment coefficient of a rotating disk*

Figure 1 shows the flow model used in the analysis. The disk is rotated at a constant angular velocity ω in a fluid of infinite extent, and there is a boundary layer on the rotating disk surface. If r, θ and z are cylindrical polar coordinates, u_r and u_θ are the velocity components of the fluid in the directions of r and θ and the axial velocity component is neglected, then the momentum integral equations of the boundary layer on the rotating disk are

$$\frac{\mathrm{d}}{\mathrm{d}r}\left(r\int_0^\delta u_r^2\,\mathrm{d}z\right)-\int_0^\delta u_\theta^2\,\mathrm{d}z=-\frac{\tau_r r}{\rho}, \tag{1}$$

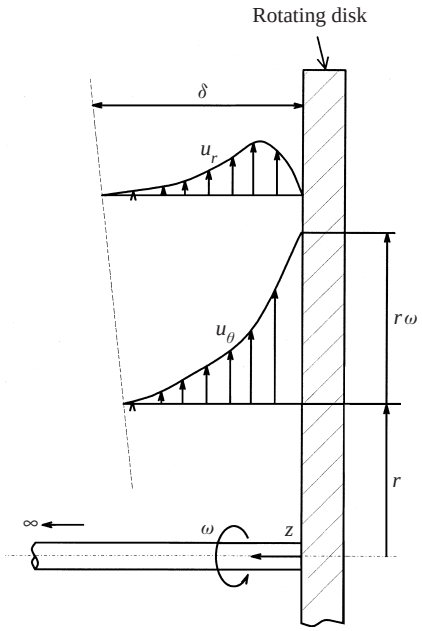

FIGURE 1. Flow model of velocity profiles in boundary layer on a rotating disk in a fluid at rest.

$$\frac{\mathrm{d}}{\mathrm{d}r}\left(r^2\int_0^{\delta} u_r u_\theta \mathrm{d}z\right) = -\frac{\tau_\theta r^2}{\rho}, \tag{2}$$

where τ_r and τ_θ are shearing stress components at the surface, δ is the boundary layer thickness, and ρ is the fluid density.

It is well known that the logarithmic velocity profiles in a circular pipe cover a wide range of Reynolds numbers. If $\tau_0 = \rho v_*^2$ represents shearing stress at a wall, and u is the velocity near the disk wall, the logarithmic velocity profile is

$$u^+ = A\log_{\mathrm{e}} y^+ + B, \tag{3}$$

where $u^+ = u/v_*$ and $y^+ = v_* z/v$.

The constants A and B are generally known semi-empirically to be $A = 2.5$ and $B = 5.5$ for Newtonian fluids, hence the logarithmic velocity profile for Newtonian fluids is

$$u^+ = 2.5\log_{\mathrm{e}} y^+ + 5.5. \tag{4}$$

Virk *et al.* (1970) obtained the ultimate velocity profiles for dilute polymer solutions, in the maximum drag-reduction range for a circular pipe as follows:

$$u^+ = 11.7\log_{\mathrm{e}} y^+ - 17 \tag{5}$$

Figure 2 shows the experimental results for velocity profiles for surfactant solutions presented in other studies (Bewersdorff & Ohlendorf 1988; Ito *et al.* 1995; Zakin *et al.* 1996; Warholic *et al.* 1999). Additionally, from their experimental data, Zakin *et al.* proposed the following equation for surfactant solutions:

$$u^+ = 23.4\log_{\mathrm{e}} y^+ - 65. \tag{6}$$

However, as shown in figure 2, the logarithmic velocity profiles in surfactant solutions are different from (6), and Zakin *et al.* suggested that (6) was not the best velocity profile. Thus, with reference to the experimental data in figure 2, the following

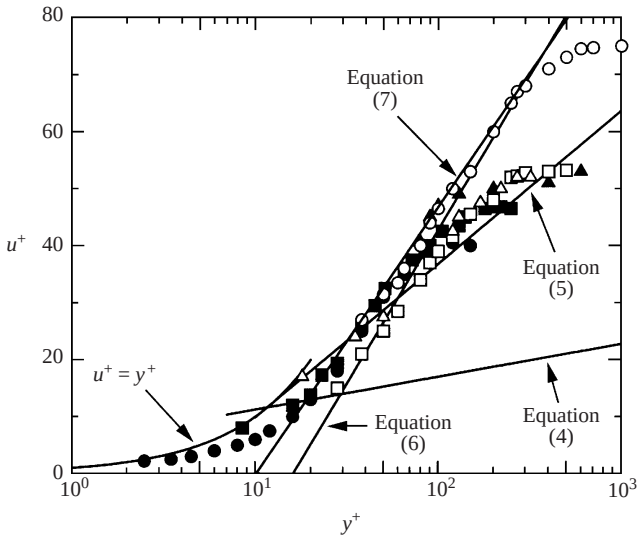

FIGURE 2. Non-dimensional velocity profiles for surfactant solutions. ○, $Re = 1.3 \times 10^5$; □, 4.1×10^4 for pipe flow (Zakin *et al.* 1996); ■, $Re = 1.5 \times 10^4$ for4 channel flow (Warholic *et al.* 1999); ●, $Re = 1.2 \times 10^4$ for channel flow (Ito *et al.* 1995); △, $Re = 2.5 \times 10^4$; ▲, 1.2×10^5 for pipe flow (Bewersdorff & Ohlendorf 1988).

equation for the logarithmic velocity profile of surfactant solutions is assumed in this study:

$$u^+ = 20.4 \log_e y^+ - 47. \tag{7}$$

It is clear that (7) agrees better with the experimental data for surfactant solutions than (6) in figure 2.

For Newtonian fluids, based on the logarithmic velocity profile of turbulent pipe flow, Goldstein (1935) and Ito (1963) reported analytical results for the moment coefficient of a rotating disk by using momentum integral equations of the boundary layer on a rotating disk. With reference to their analysis, the moment coefficient of a rotating disk in a drag-reducing surfactant solution was calculated by applying (7) for the velocity profiles of the boundary layer on the disk.

If u is the velocity near the rotating disk surface, the radial and tangential components of velocity profiles are assumed as follows (Goldstein 1935):

$$u_r = \frac{\alpha}{\sqrt{1+\alpha^2}} u, \tag{8}$$

$$u_\theta = \omega r - \frac{1}{\sqrt{1+\alpha^2}} u, \tag{9}$$

where α is a constant related to the flow direction.

The boundary conditions are

$$u_r = 0, \quad u_\theta = \omega r \quad \text{at} \quad z = 0,$$

$$u_r = 0, \quad u_\theta = 0 \quad \text{at} \quad z = 0.$$

By substituting (3) into (8) and (9), and transforming the equations to satisfy the

boundary conditions, the velocity profiles are obtained as

$$u_r = \frac{\alpha}{\sqrt{1+\alpha^2}}\left(\omega r\sqrt{1+\alpha^2} + Av_* \log_e \frac{z}{\delta}\right)\left(1-\frac{z}{\delta}\right), \tag{10}$$

$$u_\theta = -\frac{Av_*}{\sqrt{1+\alpha^2}} \log_e \frac{z}{\delta}. \tag{11}$$

The radial and tangential components of shearing stress acting on a disk wall are obtained as (Goldstein 1935)

$$\tau_r = \frac{\alpha}{\sqrt{1+\alpha^2}}\tau_0, \tag{12}$$

$$\tau_\theta = -\frac{1}{\sqrt{1+\alpha^2}}\tau_0. \tag{13}$$

By substituting (10)–(13) into (1) and (2), we obtain

$$\frac{\mathrm{d}}{\mathrm{d}r}\left[\left(\frac{1}{3} - \frac{11}{9}\frac{Av_*}{\omega r} + \frac{85}{54}\left(\frac{Av_*}{\omega r}\right)^2\right) r^3\alpha^2\delta\right] - 2\left(\frac{Av_*}{\omega r}\right)^2 r^2\delta = -\frac{1}{A^2}\left(\frac{Av_*}{\omega r}\right)^2 r^3\alpha, \tag{14}$$

$$\frac{\mathrm{d}}{\mathrm{d}r}\left[\left(\frac{3}{4}\frac{Av_*}{\omega r} + \frac{7}{4}\left(\frac{Av_*}{\omega r}\right)^2\right) r^4\alpha\delta\right] = \frac{1}{A^2}\left(\frac{Av_*}{\omega r}\right)^2 r^4. \tag{15}$$

Now, the values of functions α and δ can be assumed to be

$$\alpha = \alpha_1\frac{Av_*}{\omega r} + O\left[\left(\frac{Av_*}{\omega r}\right)^2\right], \tag{16}$$

$$\delta = \delta_0 + O\left(\frac{Av_*}{\omega r}\right)^2, \tag{17}$$

where α_1 and δ_0 are functions of r.

For large Reynolds numbers, the high-order terms involving $(Av^*/\omega r)$ are very small. Thus, these expressions may be reduced by neglecting high-order terms. By substituting (16) and (17) into (14) and (15) and neglecting the high-order terms, the equations for α_1 and δ_0 become

$$\frac{\mathrm{d}}{\mathrm{d}r} r^2\alpha_1^2\delta_0 = 6r^2\delta_0 \tag{18}$$

$$\frac{\mathrm{d}}{\mathrm{d}r}\alpha_1\delta_0 + \frac{4}{r}\alpha_1\delta_0 = \frac{4}{3A^2}, \tag{19}$$

so that

$$\alpha = \sqrt{\frac{3}{2}}\frac{Av_*}{\omega r}, \tag{20}$$

$$\delta = \frac{4}{15A^2}\sqrt{\frac{2}{3}}r. \tag{21}$$

The moment acting on one side of the disk is

$$M = -2\pi\int_0^a r^2\tau_\theta\,\mathrm{d}r = 2\pi\rho a^2\int_0^\delta u_r u_\theta\,\mathrm{d}z.$$

On evaluation of the integral forms (10), (11), (20) and (21), we find that

$$M = \frac{4\pi\rho a^5\omega^2\alpha^2}{45A^2(1+\alpha^2)}\left(3\sqrt{1+\alpha^2} - \frac{7\sqrt{2}}{\sqrt{3}}\alpha\right). \tag{22}$$

Thus, the moment coefficient acting on one side of the disk wall is

$$C_m = \frac{M}{1/2\rho\omega^2 a^5} = \frac{8\pi\alpha^2(3\sqrt{3(1+\alpha^2)} - 7\sqrt{2}\alpha}{45\sqrt{3}A^2(1+\alpha^2)}. \tag{23}$$

For the boundary condition $u = \omega r\sqrt{1+\alpha^2}$ at $z = \delta$, (3) becomes

$$\frac{\omega r\sqrt{1+\alpha^2}}{v_*} = A\log_e\frac{v_*\delta}{v} + B. \tag{24}$$

By substituting (21) and (23) into (24), we obtain the moment coefficient acting on one side of the disk from the following simple formula:

$$\frac{1}{\sqrt{C_m}} = m\log_{10}(\mathrm{Re}\sqrt{C_m}) + n, \tag{25}$$

where

$$m = \frac{A}{2}\sqrt{\frac{15\sqrt{3}}{\pi(3\sqrt{3(1+\alpha^2)} - 7\sqrt{2}\alpha)}}\log_e 10,$$

$$n = \frac{\sqrt{3}A}{2\sqrt{(1+\alpha^2)}}\sqrt{\frac{5\sqrt{3}(1+\alpha^2)}{\pi(3\sqrt{3(1+\alpha^2)} - 7\sqrt{2}\alpha)}}\left(\log_e\left(\frac{8\alpha}{45A^3}\right) + \frac{B}{A}\right)$$
$$-m\log_e 10\log_{10}\left(\frac{2\alpha}{3A}\sqrt{\frac{2\pi(3\sqrt{3(1+\alpha^2)} - 7\sqrt{2}\alpha)}{5\sqrt{3}(1+\alpha^2)}}\right),$$

and $Re = \omega r^2/v$ is the Reynolds number.

As mentioned above, α is a function related to the flow angle ϕ near the rotating disk, where $\alpha = -\tan\phi$. In this study, the value of α was assumed from experimental results for flow angle on the rotating disk. By substituting α in (25), the moment coefficient of a rotating disk can be calculated exactly.

2.2. *Flow angle*

In order to clarify the mechanism of drag reduction, it is important to elucidate the flow angle near the rotating disk. The flow angle can be considered an important physical quantity on the basis of an examination of the drag-reduction mechanism.

In general, the flow angle ϕ near the rotating disk can be written as

$$\tan\phi = -\tau_r/\tau_\theta. \tag{26}$$

Combining (12), (13), (20) and (26), we obtain

$$\tan\phi = \sqrt{\frac{3}{2}}\frac{Av_*}{\omega r}. \tag{27}$$

By substituting (21) and (27) into (24), we obtain the flow angle as a function of

A, B and Re:

$$\frac{\sqrt{1+\tan^2\phi}}{\tan\phi}\sqrt{\frac{3}{2}} = \log_e\left(\frac{8}{45}\frac{\tan\phi}{A^3}Re\right) + \frac{B}{A}. \tag{28}$$

3. Experimental results and discussion

3.1. *Moment coefficient of rotating disk*

Experiments were carried out to measure the torque acting on one side of a rotating disk in housing. Details of the experimental apparatus and results were reported by the authors in a previous paper (Ogata & Watanabe 1999). The apparatus consisted of two rotating disks: a test rotating disk and a support disk. The test rotating disk was made of aluminum, and was 180 mm in diameter and 3 mm thick. The support disk covered one side and the edge of the test disk. The two disks were rotated at the same speed in the same direction. The torque on one side of the test rotating disk was measured directly using strain gauges cemented to the top of the shaft. The clearance s between the test disk and stator was 10 mm. Test surfactant solutions were aqueous solutions of Ethoquad O/12($C_{18}H_{35}N(C_2H_4OH)_2CH_3Cl$, Lion Co.) at concentrations of 50, 100, and 200 p.p.m., and sodium salicylate ($C_7H_5NaO_3$) was added as a counterion. The experiments were performed with the temperature of the surfactant solution maintained at $t = 18$ and 28 °C.

It was confirmed that the moment coefficient on an enclosed rotating disk was reduced by surfactant solutions and that the drag reduction of the surfactant solution depended on both concentration and temperature. The maximum drag reduction ratio was approximately 30% in 200 p.p.m. Ethoquad O/12 solution at $Re = 5 \times 10^5$.

The values of the moment coefficient of a rotating disk for maximum drag reduction for several concentrations of surfactant solutions are plotted in figure 3. It can be seen that the data approximates the solid line labelled 2, $C_m = 1.85(s/a)^{-1/2}Re^{-1/2}$ (Daily & Nece 1960) for the enclosed rotating disk, for all concentrations of the surfactant solution. This suggests that the minimum value of the data for surfactant solutions did not vary in this Reynolds number range.

3.2. *Flow visualization and flow angle*

Flow visualization was performed using the tracer and the tuft techniques (Ogata & Watanabe 2000). The tracer technique was applied by mixing aluminium powder in the test solution in the approximate concentration of 0.2 mg l^{-1}. A laser unit with a slit was used to generate a flat beam (90×0.5 mm). Photographs of streaks of aluminium powder within 0.5 mm of the disk surface were captured. In the tuft technique, tufts 0.1 mm in diameter and 1.5 mm in length were cemented onto the rotating disk wall at $r = 35$, 45, 55, 65, 75, 85 mm and 48 tufts were used in total. The condition of the clearance ratio (s/a) was as in the torque measurement experiment. The disk was rotated clockwise, and the tuft pattern measured using a stroboscope.

Figures 4 and 5 show the flow visualization results from the tracer technique at Reynolds numbers of $Re = 2.5 \times 10^5$ and 3.5×10^5, respectively. The camera shutter speed was 1/60 s. Figures 4(a) and 5(a) show the flow visualization results for tap water, and figures 4(b) and 5(b) show the flow visualization results for 200 p.p.m. Ethoquad O/12 solution. The Reynolds number of the surfactant solution was calculated using the viscosity of tap water. In the case of $s/a = 0.115$, Daily & Nece (1960) reported that the transition to turbulent flow began at $Re = 2.8 \times 10^4$

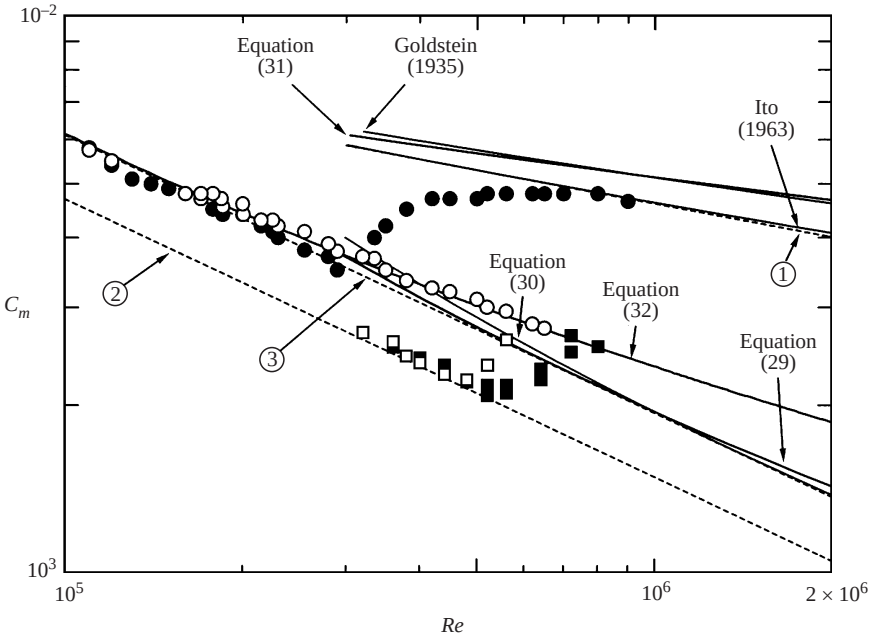

FIGURE 3. Moment coefficient of a rotating disk. □, ■, ■, Ethoquad O/12 solutions with 50, 100 and 200 p.p.m. counterion respectively (Ogata & Watanabe 1999); ○, 50 p.p.m. Separan; ●, tap water (Watanabe 1978); ①, $C_m = 0.073Re^{-1/5}$, for a free disk in turbulent flow (Kármán 1921); ②, $C_m = 1.85(s/a)^{1/10}Re^{-1/2}$, for an enclosed disk in laminar flow (Daily & Nece 1960); ③, $C_m = 1.935Re^{-1/2}$, for a free disk in laminar flow (Kármán 1921).

and that turbulence in the boundary layer began at $Re = 1.5 \times 10^5$. Thus, figures 4 and 5 represent the transition and turbulent flow ranges, respectively.

For tap water, two or three white streaks in tangential directions, are seen in figure 4(a). These streaks represent flow vortices on the rotating disk and appear in the transition to turbulent flow. In the case of the Ethoquad O/12 solution shown in figure 4(b), the streaks did not appear clearly. If the contrast between dark and light strips is strong, the vortices near the rotating disk can be considered to be powerful because the reflected light intensity of the aluminium powder indicates the strength of the flow. Therefore, the vortices in the Ethoquad O/12 solution were weaker than those in tap water. Hence, the surfactant solution reduces the amplitude of the circular vortex on a rotating disk. In addition, the flow direction near the disk is turned towards the outward direction by the surfactant solution.

The streaks are not clear in figure 5(a) because the flow was turbulent. In figure 5(b), the contrast between the dark and light stripes of the Ethoquad O/12 solution is not stronger than that of tap water. This suggests that the surfactant solution reduces the turbulent flow directional quality.

The results of flow visualization by the tuft technique are shown in figure 6. Examples of the tuft pattern for Ethoquad O/12 solution and tap water are placed side by side for the same Reynolds number $Re = 4.2 \times 10^5$, and the relative angles of tufts evaluated. The flow angles were obtained from the tangent line of the tufts, and experimental flow angle results are shown in figure 7. For comparison, the experimental results for flow angle in dilute polymer solutions are also shown (Bilgen 1971; Watanabe 1978). It can be seen that the flow angles for a surfactant solution are larger than those for a Newtonian fluid in the turbulent flow range of the Reynolds

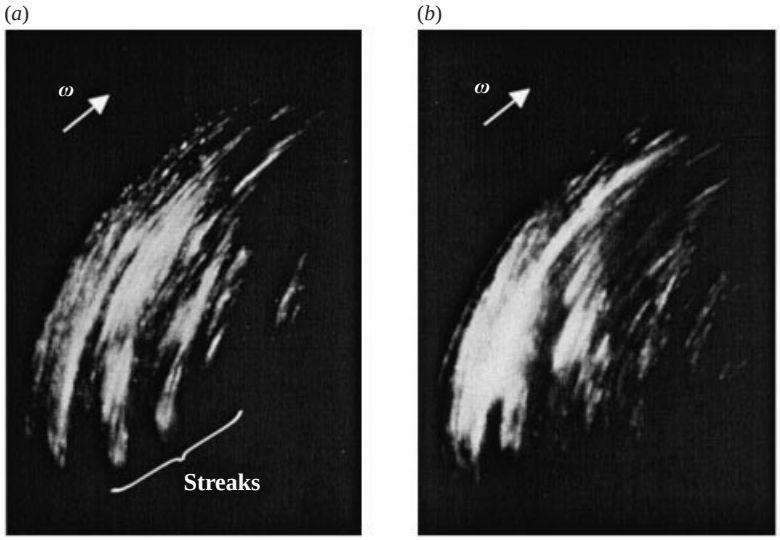

FIGURE 4. Flow patterns near a rotating disk at $Re = 2.5 \times 10^5$. (*a*) Tap water, (*b*) 200 p.p.m. Ethoquad O/12 solution.

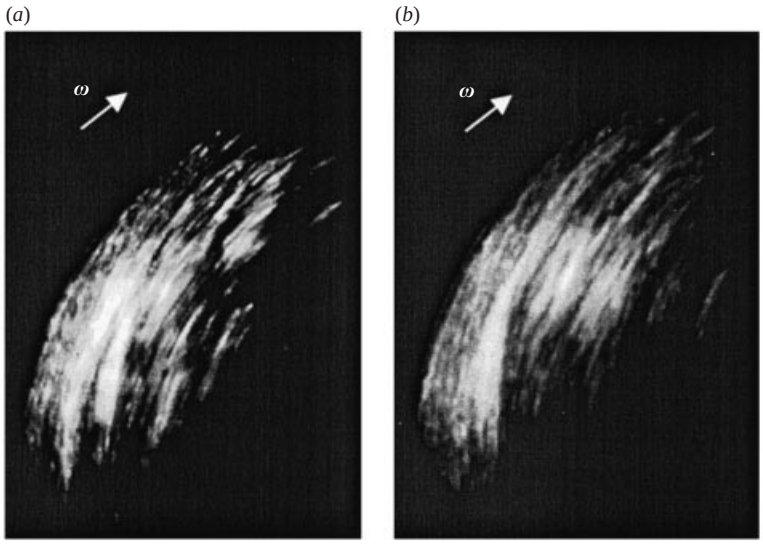

FIGURE 5. Flow patterns near a rotating disk at $Re = 3.5 \times 10^5$. (*a*) tap water, (*b*) 200 p.p.m. Ethoquad O/12 solution.

number. In other words, the flow direction near the disk is turned outwards by the surfactant solution.

Additionally, calculated results from (25) for the turbulent range of the Reynolds number are shown in figure 7. Analysis of flow angle on the rotating disk was carried out by substituting (4), (5) and (7) into (28). It is shown that the analytical results provide different flow angles for different test fluids. The calculated results decrease with increasing Reynolds number for surfactant and polymer solutions, but the results for Newtonian fluid remain constant and demonstrate no dependence on Reynolds number. It is seen that the experimental results for surfactant and polymer solutions

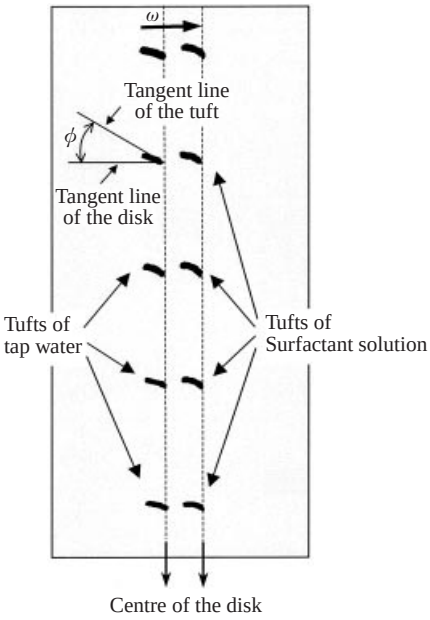

FIGURE 6. Examples of tuft patterns of surfactant solution and tap water under identical conditions.

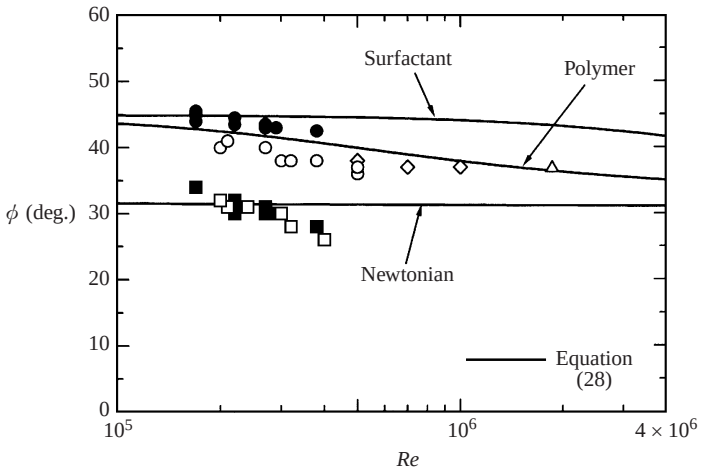

FIGURE 7. Flow angles on a rotating disk. ●, ■, Present data, surfactant and tap water, respectively; ○, □, Separan AP30 and tap water for a free disk, respectively; ◇, Separan AP30 for an enclosed disk (Watanabe 1978); △, Separan AP 273 (Bilgen 1971).

agree well with the analytical results in the range $Re < 7 \times 10^5$, and it was clarified that the flow angles for a surfactant solution are larger than those for a polymer solution.

Consequently, the increased flow angle on the rotating disk and decreased amplitude of a circular vortex due to surfactant solutions led to drag reduction for the rotating disk.

	Surfactant		Polymer	Newtonian		
	Eq. (29)	Eq. (30)	Eq. (32)	Eq. (31)	Goldstein (1935)	Ito (1963)
m	16.2	18.7	10	2.4	2.78	3.51
n	−52.6	−64.0	−26.2	2.3	0.46	−2.26

TABLE 1. Comparison of parameters in (25): $1/\sqrt{C_m} = m\log_{10}(\mathrm{Re}\sqrt{C_m}) + n$

3.3. *Limiting maximum drag-reduction asymptote*

The limiting maximum drag-reduction asymptote for the moment coefficient of a free disk in a surfactant solution based on the experimental results for the moment coefficient of a rotating disk and flow angle will be derived in this section.

As shown in figure 7, the flow angle on the disk for a surfactant solution decreases gradually with increasing Reynolds number. However, for simplification, we assume a flow angle of $\phi = 45^\circ$ from the experimental and analytical results such that $\alpha = -1$.

By substituting the coefficients $A = 20.4$; $B = -47$ of (7) and $\alpha = -1$ into (25), we obtain the values $m = 16.2$ and $n = -74.7$. Goldstein (1935) suggested that it is necessary to modify the values of m and n using experimental data, since the velocity profiles of the boundary layer are approximated by the velocity profiles of circular pipe flow.

Little experimental data exists for a free disk in the case of surfactant solutions. It is well known that the value of the moment coefficient of an enclosed rotating disk decreases by approximately one-half since the fluid in the chamber rotates at approximately one-half of the angular velocity of the disk in this Reynolds number range. Therefore, in this study, experimental data for a free rotating disk are correlated with those for an enclosed rotating disk.

When the coefficient is corrected by assuming that the experimental result for surfactant solution approximates the solid line labelled 2 in figure 3, we obtain the formula of the limiting maximum drag-reduction asymptote for the moment coefficient of a rotating disk in a surfactant solution:

$$\frac{1}{\sqrt{C_m}} = 16.2\ \log_{10}(\mathrm{Re}\sqrt{C_m}) - 52.6. \tag{29}$$

Equation (29) is shown in figure 3, and is seen to agree with data for surfactant solutions, even if the parameter m is not modified. As mentioned above, (29) is not directly comparable with the experimental results for the enclosed rotating disk. However, in figure 3, (29) shows the behaviour of the moment coefficient of the free disk in a surfactant solution.

For comparison, in the case of the velocity profile of a surfactant solution given in (6), the same calculation procedure was followed. These calculated results are shown in table 1, and the formula using (6) was as follows:

$$\frac{1}{\sqrt{C_m}} = 18.7\ \log_{10}(\mathrm{Re}\sqrt{C_m}) - 64. \tag{30}$$

It is seen in figure 3 that the moment coefficient of (30) is smaller than that of (29) in the large Reynolds number range, but the difference may be very small in the Reynolds number range $Re < 2 \times 10^6$.

The moment coefficient of a rotating disk in a Newtonian fluid was calculated in the same manner as that in a surfactant solution. By substituting the coefficients of (4) into (25), and assuming a flow angle of $\phi = 30°$, we obtain $m = 2.4$ and $n = -2.0$. Modifying the coefficient of n using Kármán's turbulent flow formula (curve 1 in figure 3) $C_m = 0.073\,Re^{-1/5}$ (von Kármán 1921), we obtain the moment coefficient for Newtonian fluid as follows:

$$\frac{1}{\sqrt{C_m}} = 2.4\,\log_{10}(Re\sqrt{C_m}) + 2.3. \tag{31}$$

Equation (31) is also shown in figure 3. Goldstein (1935) and Ito (1963) obtained the formulae for the moment coefficient for a Newtonian fluid by modifying both coefficients m and n based on experimental data. Table 1 shows a comparison of these coefficients. The formulae are also shown in figure 3. It is seen that (31) agrees well with Goldstein's formula in the range $10^5 < Re < 2 \times 10^6$.

In order to ascertain the significance of the maximum drag-reduction asymptote for a surfactant solution, it is necessary to obtain a corresponding equation for a dilute polymer solution in which the drag reduction of a rotating disk occurred as in (29). For dilute polymer solutions, Watanabe (1978) reported experimental data for the moment coefficient of a disk in a large tank. The experimental results for the maximum drag reduction are shown in figure 3. The flow angle of the polymer solution is assumed to be $\phi = 40°$ from experimental results in previous studies and results presented in this study. By substituting (5) and $\phi = 40°$ into (25), we obtain $m = 10$ and $n = -37$. Modifying the coefficient n using experimental results for maximum drag-reduction, we also obtain the formula of the limiting maximum drag-reduction asymptote for the moment coefficient of a rotating disk in a dilute polymer solution:

$$\frac{1}{\sqrt{C_m}} = 10\log_{10}(Re\sqrt{C_m}) - 26.2. \tag{32}$$

As shown in figure 3, good agreement between experimental data and (32) is obtained in the range $Re < 7 \times 10^5$.

It can be seen that the moment coefficient for a surfactant solution decreases compared with that of a dilute polymer solution, and the tendency is similar to that of pipe flow.

As a result of this analysis, a linear relationship between the coefficient α in (3) and m in (25) is found, and m does not require modification by experimental results. This suggests that the slope of the moment coefficient can be calculated directly using the slope of the logarithmic velocity profiles of pipe flow. Thus, it can be considered that the slope of the moment coefficient represents the limit of the drag reduction due to surfactant solutions.

4. Conclusions

The limiting maximum drag-reduction asymptote for the moment coefficient of a rotating disk was obtained analytically in drag-reducing surfactant solutions and polymer solutions. Analysis was carried out using momentum integral equations of the boundary layer on a rotating disk based on the logarithmic velocity profile of turbulent pipe flow. The analytical results agreed quantitatively with experimental results of maximum drag reduction for surfactant and polymer solutions. It has been shown that the moment coefficient for a surfactant solution decreases compared with that of a dilute polymer solution.

Flow visualization was performed using the tracer and tufts techniques. It was clarified that the amplitude of a circular vortex of surfactant solution decreased and the flow near the disk wall was turned towards the circumferential direction in the transition to turbulent flow range. The results show that the flow angles of a rotating disk in surfactant solution were larger than those in Newtonian fluids; and the experimental results could be explained by the analytical result.

Consequently, an increased flow angle on the rotating disk and a decreased amplitude of the circular vortex due to the surfactant solution led to drag reduction for the rotating disk.

This research was supported a Grant-in-Aid for the Encouragement of Young Scientists, No. 12750145 from the Scientific Research Fund of the Japanese Government.

REFERENCES

Bewersdorff, H. W. & Ohlendorf, D. 1988 The behaviour of drag-reducing cationic surfactant solution. *Colloid Polymer Sci.* **266**, 941–953.

Bilgen, E. 1971 Stability of three-dimensional boundary layer of dilute polymer solutions. *Trans. ASME: J. Basic Engng* **93**, 85–87.

Daily, J. W. & Nece, R. E. 1960 Chamber dimension effects on induced flow and frictional resistance of enclosed rotating disks. *Trans. ASME: J. Basic Engng* **82**, 217–232.

Goldstein, S. 1935 On the resistance to the rotation of a disc immersed in a fluid. *Proc. Camb. Phil. Soc.* **31**, 232–241.

Ito, H. 1963 Frictional resistance formula of a rotating disk. *Rep. Inst. High Speed Mech. Tohoku Univ. Japan* **19**(185), 83–111 (in Japanese).

Ito, M., Imao, S. & Sugiyama, K. 1995 Characteristics of low-speed streaks in the flow of drag-reducing surfactant solution. *Trans JSME.* **61**(590B), 3664–3670 (in Japanese).

von Kármán, Th. 1921 Über laminare und turbulente Reibung. *Z. Angew. Math. Mech.* **1**, 233–252.

Kawaguchi, Y., Tawaraya, Y., Yabe, A., Hishida, K. & Maeda, M. 1996 Active control of turbulent drag reduction in surfactant solution. *Proc. ASME Fluid Engng Div. Summer Meeting*. FED-237, vol. 2, pp. 47–52.

Ogata, S. & Watanabe, K. 1999 Drag reduction of surfactant solutions for an enclosed rotating disk. *Proc. Intl ASME Rheology and Fluid Mechanics of Nonlinear Materials*. FED-249, pp. 15–19.

Ogata, S. & Watanabe, K. 2000 Flow characteristics of a rotating disk in surfactant solutions. *Proc. Intl ASME Rheology and Fluid Mechanics of Nonlinear Materials*. FED-252, pp. 41–48.

Ohlendorf, D., Interthal, W. & Hoffmann, H. 1986 Surfactant systems for drag reduction: physico-chemical; properties and rheological behavior. *Rheologica Acta.* **25**, 468–486.

Usui, H., Ito, T. & Saeki, T. 1996 Drag reducing pipe flow of surfactant solutions *Proc. ASME Fluid Engng Div. Summer Meeting*. FED-237, vol. 2, pp. 159–163.

Virk, P. S., Mickley, H. S. & Smith, K. A. 1970 The ultimate asymptote and mean flow structure in Tom's phenomenon. *Trans. ASME: J. Appl. Mech.* **37**, 488–493.

Warholic, M. D., Schmidt, G. M. & Hanratty, T. J. 1999 The influence of a drag-reducing surfactant on a turbulent velocity field. *J. Fluid Mech.* **388**, 1–20.

Watanabe, K. 1978 Frictional resistance of a rotating disk in polymer solutions. *Bull. JSME* **21**(153), 455–462.

Zakin, J. L. & Chang, J. L. 1974 Polyoxyethylene alcoholnon-ionic surfactants as drag reducing additives. *Proc. Intl Conf. on Drag Reduction*, D1, pp. 1–14.

Zakin, J. L., Myska, J. & Chara, Z. 1996 New limiting drag reduction and velocity profile asymptotes for nonpolymeric additives systems. *AIChE J.* **42**, 3544–3546.